Homology of the mapping class group $\Gamma_{2,1}$ for surfaces of genus 2 with a boundary curve

JOCHEN ABHAU

CARL-FRIEDRICH BÖDIGHEIMER

RALF EHRENFRIED

We report on the computation of the integral homology of the mapping class group $\Gamma_{g,1}^m$ of genus g surfaces with one boundary curve and m punctures, when $2g+m\leq 5$, in particular $\Gamma_{2,1}^0$.

Dedicated to the memory of Heiner Zieschang

1　Introduction

Let $\mathfrak{Mod} = \mathfrak{Mod}_{g,n}^m$ denote the moduli space of conformal equivalence classes of Riemann surfaces $F = F_{g,n}^m$ of genus $g \geq 0$ with $n \geq 1$ boundary curves and $m \geq 0$ permutable punctures. One obtains an $(m!)$–fold covering space $\widetilde{\mathfrak{Mod}} = \widetilde{\mathfrak{Mod}}_{g,n}^m$ of $\mathfrak{Mod} = \mathfrak{Mod}_{g,n}^m$ if the punctures are declared not permutable.

Likewise, let $\Gamma = \Gamma_{g,n}^m$ be the corresponding mapping class group of isotopy classes of orientation-preserving diffeomorphisms fixing the boundary pointwise and possibly permuting the punctures. The mapping class group where the punctures are to be fixed is a subgroup of index $m!$ in Γ and is denoted by $\widetilde{\Gamma} = \widetilde{\Gamma}_{g,n}^m$.

The main result of this article is the computation of the integral homology $H_*(\Gamma_{2,1}^0; \mathbb{Z})$ and $H_*(\Gamma_{2,1}^1; \mathbb{Z})$ of the mapping mapping class group for surfaces of genus 2 with one boundary curve and with no (respectively, one) puncture. These computations were done some years ago by the third author in [13] and redone by the first author in [1], both based on work by the second author in [6] and [5]. We give this belated report, because very few homology groups of mapping class groups are known; prior to our computations the integral homology was known only for the easy case $g = 1$. See Section 2 for more remarks on previously known results.

Γ and $\widetilde{\Gamma}$ are torsion-free, since the diffeomorphisms are fixing at least one boundary curve. They act therefore freely on the contractible Teichmüller spaces $\mathfrak{Teich} = \mathfrak{Teich}_{g,n}^m$

(respectively, $\widetilde{\mathfrak{Teich}} = \widetilde{\mathfrak{Teich}}^{m}_{g,n}$). It follows, that the space $\mathfrak{Mod}$ is a non-compact, connected (topological) manifold of dimension $d = 6g - 6 + 3n + 2m$; the manifold $\widetilde{\mathfrak{Mod}}$ is always orientable, but $\mathfrak{Mod}$ is orientable only in the cases $m = 0$ or $m = 1$. Furthermore, they have the homotopy type of the classifying space of the corresponding mapping class group,

$$(1\text{--}1) \qquad \begin{array}{ccccc} \widetilde{\mathfrak{Mod}} & =\!=\!= & \widetilde{\mathfrak{Teich}}/\widetilde{\Gamma} & \xrightarrow{\;\simeq\;} & B\widetilde{\Gamma} \\ \downarrow & & \downarrow & & \downarrow \\ \mathfrak{Mod} & =\!=\!= & \mathfrak{Teich}/\,\Gamma & \xrightarrow{\;\simeq\;} & B\Gamma \end{array}$$

The key point of our method is to use a new description of the moduli space $\mathfrak{Mod}$ (respectively, $\widetilde{\mathfrak{Mod}}$); this is the space of parallel slit domains, the space of configurations of h pairs of parallel, semi-infinite slits in n complex planes; here $h = 2g + m + 2n - 2$.

More precisely, there is a vector bundle $\mathfrak{Harm} \to \mathfrak{Mod}$ (respectively, $\widetilde{\mathfrak{Harm}} \to \widetilde{\mathfrak{Mod}}$) of dimension $d^* = m + 2n$, and its one-point-compactification will be described by parallel slit domains.

To describe these bundles we first replace the moduli spaces above by the moduli space of closed Riemann surfaces F of genus g, on which n so-called dipole points $Q_1, \ldots, Q_n$ with non-zero tangent vectors $X_1, \ldots, X_n$, and m permutable (respectively, non-permutable) punctures $P_1, \ldots, P_m$ are specified. A conformal equivalence class is given by $[F, \mathcal{Q}, \mathcal{P}, \mathcal{X}]$, with $\mathcal{Q} = (Q_1, \ldots, Q_n)$, $\mathcal{P} = (P_1, \ldots, P_m)$, and $\mathcal{X} = (X_1, \ldots, X_n)$. These new moduli spaces have the same homotopy type as $\mathfrak{Mod}$ (respectively, $\widetilde{\mathfrak{Mod}}$) or, in other words, the mapping class groups are isomorphic. Note that their dimension is $d = 6g - 6 + 4n + 2m$, since for the sake of simplicity we specified tangent vectors and not merely tangent directions.

In the vector bundle $\mathfrak{Harm} \to \mathfrak{Mod}$ (respectively, $\widetilde{\mathfrak{Harm}} \to \widetilde{\mathfrak{Mod}}$) the fibre over a point $[F, \mathcal{Q}, \mathcal{P}, \mathcal{X}]$ in $\mathfrak{Mod}$ (respectively, in $\widetilde{\mathfrak{Mod}}$) consists of all harmonic functions $u \colon F \to \bar{\mathbb{R}} = \mathbb{R} \cup \infty$ with a simple pole at each Q_i having direction X_i plus a logarithmic singularity, and with a logarithmic singularity at each P_j. The bundle $\mathfrak{Harm}$ is flat, more precisely $\mathfrak{Harm} \cong (\widetilde{\mathfrak{Mod}} \times_{\mathfrak{S}_m} \mathbb{R}^m) \times \mathbb{R}^{3n}$, and the bundle $\widetilde{\mathfrak{Harm}}$ is trivial, being the pullback of $\mathfrak{Harm}$ along the covering $\widetilde{\mathfrak{Mod}} \to \widetilde{\mathfrak{Mod}}/\mathfrak{S}_m = \mathfrak{Mod}$, where $\mathfrak{S}_m$ is the mth symmetric group.

In [5] we have (following an earlier version in [6]) introduced a finite cell complex $\mathrm{Par} = \mathrm{Par}(h, m, n)$ of dimension $d + d^* = 3h$ as a compactification of $\mathfrak{Harm}$. The complement of $\mathfrak{Harm}$ is a subcomplex $\mathrm{Par}' \subset \mathrm{Par}$ of codimension 1 and its points represent degenerate surfaces. A similar statement holds for $\widetilde{\mathfrak{Harm}}$. The main result in

[5] and Ebert [11] is

$$(1\text{–}2) \qquad \mathrm{Par} - \mathrm{Par}' \quad \cong \quad \mathfrak{Harm} \quad \simeq \quad \mathfrak{Mod},$$

$$(1\text{–}3) \qquad \widetilde{\mathrm{Par}} - \widetilde{\mathrm{Par}}' \quad \cong \quad \widetilde{\mathfrak{Harm}} \quad \simeq \quad \widetilde{\mathfrak{Mod}}.$$

We later give some details when we exhibit the cellular chain complexes.

The pairs $(\mathrm{Par}, \mathrm{Par}')$ (respectively, $(\widetilde{\mathrm{Par}}, \widetilde{\mathrm{Par}}')$) are relative manifolds, and via Poincaré duality we obtain the isomorphisms:

$$(1\text{–}4) \qquad H^*(\mathrm{Par}, \mathrm{Par}'; \mathcal{O}) \cong H_{3h-*}(\mathfrak{Mod}; \mathbb{Z}),$$

$$(1\text{–}5) \qquad H^*(\widetilde{\mathrm{Par}}, \widetilde{\mathrm{Par}}'; \mathbb{Z}) \cong H_{3h-*}(\widetilde{\mathfrak{Mod}}; \mathbb{Z})$$

These isomorphisms are the cap-product with a (relative) fundamental or orientation class $[\mu]$ in $H^{3d}(\mathrm{Par}, \mathrm{Par}'; \mathcal{O})$ (respectively, in $H^{3d}(\widetilde{\mathrm{Par}}, \widetilde{\mathrm{Par}}'; \mathbb{Z})$) where $\mathcal{O}$ is the local coefficient system induced by the orientation covering.

In the following sections we concentrate for the sake of simplicity on the case of a single boundary curve ($n = 1$), although the computations can be done in the general case. To compute the homology of $\mathfrak{Mod}$ and $\widetilde{\mathfrak{Mod}}$ we actually computed the cellular homology of the pairs $(\mathrm{Par}, \mathrm{Par}')$ with integral, with mod 2 and with rational coefficients, and with coefficients in the orientation system $\mathcal{O}$. The actual calculations were done using a computer program; the program is not tracking the generators of the homology groups, but some generators can easily be determined.

In Section 2 we will list our results. We will give comments on previous and similar homology computations. We give a description of the spaces $\mathfrak{Harm}$ and $\widetilde{\mathfrak{Harm}}$ in Section 3, including figures of configurations, that is, parallel slit domains; in particular we give a complete list of cells for the case $g = 1$ and $m = 0$, which we will use in Section 6 for a demonstration. In Section 4 we describe the cellular chain complexes. Some properties of these chain complexes are described in Section 5. The calculation for the case $g = 1$ and $m = 0$ is done by hand in Section 6 to demonstrate the method, in particular the spectral sequence used. For the fundamental class μ and for some other homology classes we can give formulas (for their Poincaré) duals in Section 7. The orientation system is described in Section 8. And we comment on the computer program in Section 9.

Acknowledgements

2 Results

2.1 The permutable case

We present our results in the form of a table. It shows all non-trivial integral homology groups of the moduli space $\mathfrak{Mod}$ for $h \leq 5$ and $g > 0$ and $n = 1$.

$* =$	0	1	2	3	4	5	6
$H_*(\mathfrak{Mod}^0_{1,1}; \mathbb{Z}) =$	$\mathbb{Z}$	$\mathbb{Z}$					
$H_*(\mathfrak{Mod}^1_{1,1}; \mathbb{Z}) =$	$\mathbb{Z}$	$\mathbb{Z}$	$\mathbb{Z}/2$				
$H_*(\mathfrak{Mod}^2_{1,1}, \mathbb{Z}) =$	$\mathbb{Z}$	$\mathbb{Z}\oplus\mathbb{Z}/2$	$\mathbb{Z}/2\oplus\mathbb{Z}/2$	$\mathbb{Z}/2$			
$H_*(\mathfrak{Mod}^3_{1,1}; \mathbb{Z}) =$	$\mathbb{Z}$	$\mathbb{Z}\oplus\mathbb{Z}/2$	$\mathbb{Z}/2\oplus\mathbb{Z}/2$	$\mathbb{Z}\oplus\mathbb{Z}/2\oplus\mathbb{Z}/2$	$\mathbb{Z}$	$\mathbb{Z}$	
$H_*(\mathfrak{Mod}^0_{2,1}; \mathbb{Z}) =$	$\mathbb{Z}$	$\mathbb{Z}/10$	$\mathbb{Z}/2$	$\mathbb{Z}\oplus\mathbb{Z}/2$	$\mathbb{Z}/6$		
$H_*(\mathfrak{Mod}^1_{2,1}; \mathbb{Z}) =$	$\mathbb{Z}$	$\mathbb{Z}/10$	$\mathbb{Z}\oplus\mathbb{Z}/2$	$\mathbb{Z}\oplus\mathbb{Z}\oplus\mathbb{Z}/2\oplus\mathbb{Z}/2$	$\mathbb{Z}/6\oplus\mathbb{Z}/6$	$\mathbb{Z}$	$\mathbb{Z}$

2.2 Remarks

(1) For $g = 0$, the moduli spaces $\mathfrak{Mod}^m_{0,1}$ are the unordered configuration spaces of m points in a disk or in the plane. The mapping class group $\Gamma^m_{0,1}$ is the (Artin) braid group $\mathrm{Br}(m)$ on m strings. Their homology is well-known and therefore we did not include the five cases $g = 0$, $h = 0, \ldots, 5$ in the table above. See Arnol'd [2; 3], Fuks [14], Vaĭnšteĭn [37] and Cohen [9; 10].

(2) The moduli space $\mathfrak{Mod}^0_{1,1}$ of the torus with one boundary curve is homotopy equivalent to the complement of the trefoil knot in $\mathbb{S}^3$. The mapping class group $\Gamma^0_{1,1}$ is a central extension

(2–1) $$1 \to \mathbb{Z} \to \Gamma^0_{1,1} \to \mathrm{SL}_2(\mathbb{Z}) \to 1$$

of $\mathrm{SL}_2(\mathbb{Z})$ by the integers and isomorphic to the third braid group $\mathrm{Br}(3)$. This central extension is a special case of the central extension

(2–2) $$1 \to \mathbb{Z}^n \to \widetilde{\Gamma}^m_{g,n} \to \widetilde{\Gamma}^{n+m}_{g,0} \to 1.$$

Here the boundary curve is turned into a puncture by gluing-in a disc. The connection to the sequence before is disguised by the fact $\widetilde{\Gamma}^0_{1,0} = \Gamma^0_{1,0} = \Gamma^1_{1,0}$, because a torus is an abelian variety; in this special case we have $\Gamma^0_{1,0} = \Gamma^1_{1,0} = \mathrm{SL}_2(\mathbb{Z})$.

(3) The computations of $H_*(\mathfrak{Mod}^0_{2,1})$ were done by the third author [13] some years ago, and redone by the first author in [1]. Very recently, Godin [17] has obtained these results independently, using a different method of computation.

(4)   Note that very little is known about the (integral) homology of a single mapping class group.

(a)   Known are the first homology groups $H_1(\Gamma_{g,n}^m)$ for all values of g, n, m. Apart from the classical case $g = 1$, this was proved by Mumford in [31] ($g = 2, n = m = 0$) and by Powell in [33] ($g \geq 3, n = m = 0$), which both use representations of the mapping class groups. For the other values of n and m one can use the extensions

(2–3) $$1 \to \mathbb{Z}^n \to \Gamma_{g,n}^m \to \Gamma_{g,0}^{n+m} \to 1$$

(2–4) $$1 \to \mathrm{Br}_k(F_{g,n}^m) \to \Gamma_{g,n}^m \to \Gamma_{g,n}^{m+k} \to 1$$

(2–5) $$1 \to \widetilde{\Gamma}_{g,n}^m \to \Gamma_{g,n}^m \to \mathfrak{S}_m \to 1$$

or argue again via representations. In the second extension $\mathrm{Br}_k(F) = \pi_1(C^k(F))$ is the kth braid group of the surface F, the fundamental group of the kth unordered configuration space $C^k(F)$. See Korkmaz [25] for a survey.

(b)   Also known are the second homology groups $H_2(\Gamma_{g,n}^m)$ by work of Harer [18]; see also the corrections by Harer [19] and Morita [29]. These computations are based on the curve complex. For a proof using presentations see Pitsch [32] and Korkmaz–Stipsicz [26].

(c)   For the third homology group $H_3(\Gamma_{g,n}^m; \mathbb{Q})$ the reference is Harer [22].

(5)   The stable mapping class groups $\Gamma_{\infty,n}^m$, that is, the limit of the mapping class groups for the genus tending to infinity, can be defined for surfaces with boundary curves: gluing on a torus with two boundary curves embeds $\Gamma_{g,n}^m$ into $\Gamma_{g+1,n}^m$. This embedding induces a homology isomorphism in degrees $\leq (g-1)/3$. This is Harer's stability theorem, see [19], and [23]. Likewise, gluing a disc onto a boundary curve and recording its center as a new puncture gives a surjection of mapping class groups $\Gamma_{g,n+1}^m \to \Gamma_{g,n}$; see the extension (2–3) above. This surjection induces also a homology isomorphism in degrees $\leq g/3$; see [21].

The proof of the Mumford conjecture by Madsen and Weiss [28] determines the homology of the stable mapping class group with rational coefficients. Using this, Galatius [15] has computed the mod–p homology of the stable mapping class group.

Note that none of our computations belong to the stable range.

(6)   The mapping class groups for surfaces with (respectively, without) boundary are quite different. The former are torsion-free groups, and have finite-dimensional classifying spaces, which can be chosen to be manifolds. Thus there homology is of finite type. In contrast, the mapping class groups of surfaces without boundary contain

elements of finite order. Thus their classifying spaces can not be finite-dimensional. Nevertheless, they have finite virtual homological dimension by a theorem of Harer [20]. In the homology of mapping class groups without boundary Glover–Mislin [16] have found torsion elements by considering finite subgroups.

(7) For homology computations with field coefficients see for example the work of Benson and Cohen [4], and the second author, Cohen and Peim [8], for $\Gamma_{2,0}^0$ with coefficients in the field $\mathbb{F}_p$ and $p = 2, 3, 5$; or see the work of Looijenga [27] for $\Gamma_{3,0}^0$ and $\Gamma_{3,0}^1$, and the work of Tommasi [35; 36] for $\Gamma_{3,0}^2$ and $\Gamma_{4,0}^0$, all with rational coefficients.

(8) The Hilbert uniformization method can also be used to parametrize the moduli spaces of surfaces with incoming and outgoing boundary curves, see [7].

(9) This uniformization method can also be used for moduli spaces of non-orientable surfaces (Kleinian surfaces); see the work of Ebert [12] and Zaw [38]. One needs besides the *oriented* slit pairs (or handles) we use here a second kind, namely the *unoriented* slit pairs (or cross-caps). In [38] the resulting cell decomposition of the moduli space was used to calculate the homology of non-orientable mapping class groups; see also Korkmaz [24].

2.3 The non-permutable case

Obviously, $\widetilde{\mathfrak{Mod}}_{g,n}^m = \mathfrak{Mod}_{g,n}^m$ for $m = 0$ and $m = 1$.

For $g = 0$ the moduli space $\widetilde{\mathfrak{Mod}}_{0,1}^m$ is the mth ordered configuration space of a disk or a plane. And the mapping class group $\widetilde{\Gamma}_{0,1}^m$ is the pure (Artin) braid group $\mathrm{Br}(m)$ on m strings. As before, their homology is well-known (see for example Arnol'd [2]) and therefore we did not include the cases $g = 0$ and $m = 0, \dots, 5$ in this table.

Thus there are for $h \le 5$ only the cases $g = 1$, $m = 2$ and $g = 1$, $m = 3$. With the available capacities we could only finish the computations for the first case, which is listed below. See Section 9 for comments.

$* =$	0	1	2	3	4
$H_*(\widetilde{\mathfrak{Mod}}_{1,1}^2; \mathbb{Z}) =$	$\mathbb{Z}$	$\mathbb{Z}$	$\mathbb{Z}/2 \oplus \mathbb{Z}/2 \oplus \mathbb{Z}/2$	$\mathbb{Z}$	$\mathbb{Z}$

3 Parallel slit domains

3.1 Dissecting a surface

We shall give here a brief description of the Hilbert uniformization, thereby concentrating on the case $n = 1$ and on the permutable case.

The Hilbert uniformization associates to a point in $\mathfrak{Harm}$ a so-called parallel slit domain. Consider on the surface $\mathcal{F} = [F, \mathcal{Q}, \mathcal{X}, \mathcal{P}]$ a harmonic function $u\colon F \to \bar{\mathbb{R}} = \mathbb{R} \cup \infty$ with exactly one dipole singularity at the point Q_1 and logarithmic singularities at the punctures $P_1, \ldots, P_m$. More precisely, for a local chart z with $z(Q_1) = 0$ and $dz(X_1) = 1$ we require that for some positive real number A_1 and B_1 the function $u(z) - A_1 \mathrm{Re}(1/z) - B_1 \mathrm{Re}(\log(z))$ is harmonic, and further that for a local chart z with $z(P_i) = 0$ we require that the function $u(z) - C_i \mathrm{Re}(\log(z))$ is harmonic. Obviously, the residues of these singularities must satisfy the equation $-B_1 + C_1 + \cdots + C_m = 0$. The set of these auxiliary parameters is the fibre of the vector bundle $\mathfrak{Harm} \to \mathfrak{Mod}$ over the point $\mathcal{F}$. Note that the function u is – up to a constant – uniquely determined by $\mathcal{F}$ and the auxiliary parameters.

This function u will have up to h critical points $S_1, S_2, \ldots$, where $u(z) = \mathrm{Re}(z^{l_k})$, for $l_k \geq 2$, in some local chart. The sum of the indices $\mathrm{ind}(S_k)$ plus the index -2 at the dipole Q_1 must be the Euler characteristic $\chi = 2 - 2g + m$.

The stable critical graph $\mathcal{K}$ consists of the vertices Q_1 and $S_1, S_2, \ldots$, and all gradient curves of u leaving critical points (to either go to Q_1 or to another critical point) as edges. Its complement $F_0 = F - \mathcal{K}$ is simply-connected. Thus u is on F_0 the real part of a holomorphic map $w = u + \sqrt{-1}v\colon F_0 \to \mathbb{C}$. Note that w is unique up to a constant.

3.2 Parallel slit domains

The image of w is the complex plane cut along horizontal slits starting at some point and running towards infinity on the left. This is called a *parallel slit domain* in geometric function theory. These slits come - generically - in pairs, suitably interlocked.

To see this, let us assume that u is generic, that is (1) that u is locally a Morse function $(\mathrm{ind}(S_1) = \mathrm{ind}(S_2) = \cdots = 1)$, (2) that the critical values are all distinct, and (3) that a gradient curve leaving a critical point does not enter another critical point, but runs to the dipole Q_1.

For $g = 1, n = 1, m = 0$ there are two generic configurations; see the following figures. For $g = 2, n = 1, m = 0$ there are 504 generic configurations; Figure 1 shows such an example. The letters $A, \ldots, H$ indicate the boundary identifications: the right bank of a slit is glued to the left bank of the paired slit. The function u corresponds to the real part. The dipole point corresponds to infinity.

Figure 2 shows two generic configurations with two pairs of slits; but since the interlocking pattern is different, for the left configuration $g = 1$, $m = 0$, whereas for the right one $g = 0$, $m = 2$.
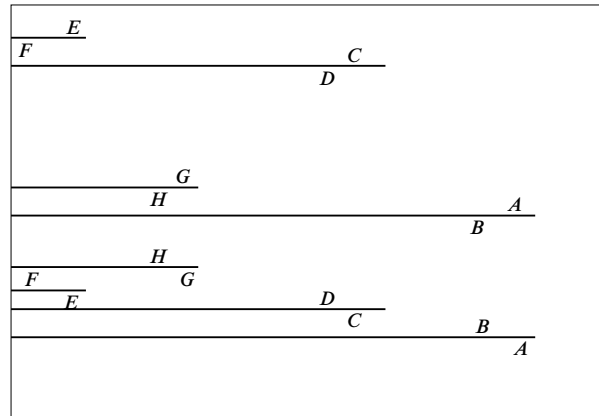
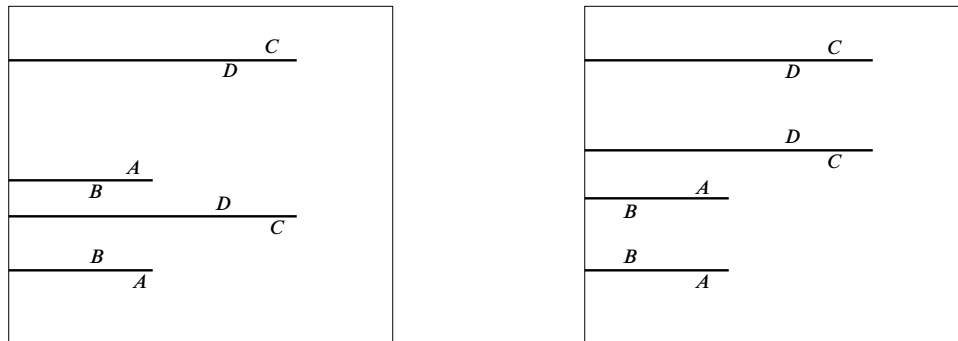Figure 1: An example of a generic parallel slit domain with $g = 2$, $m = 0$ and $n = 1$

Figure 2: Two examples of generic parallel slit domains with two pairs of slits: the different interlocking patterns give $g = 1, m = 0$ for the configuration on the left, and $g = 0, m = 2$ for the configuration on the right

3.3 Configurations and cells

If we identify the real line with an interval, the vertical and horizontal distances between the slits are two systems of (barycentric) coordinates. In other words, a top-dimensional cell is a product $\Delta^{2h} \times \Delta^h$ of two simplices, where $h = 2g + m$ is the number of pairs of slits.

In the non-generic case, the slits may have equal length, and may touch each other; in the latter case a shorter slit can jump to the other side of the partner of the longer slit pair. See the rows in Figure 6 for examples of such jumps. This leads to identifications

among faces of top-dimensional cells. Furthermore, not all configurations are allowed, since they may lead to surfaces with singularities or to surfaces with too small a genus or too few punctures. Both types of cells are called degenerate and will be excluded from the space $\mathfrak{Harm}$.

We refer the reader to [5] for details.

Figure 3 shows how the combinatorial type of these two configurations are codified. The horizontals of the slits and the verticals at the slit ends give a grid; we number the columns $0, 1, \ldots, q \leq 2$ from right to left, and the rows $0, 1, \ldots, p \leq 4$ from bottom to top. Note that in general $q \leq h$ and $p \leq 2h$. Let $R_{i,j}$ denote the jth rectangle in the ith column.

For the ith column let σ_i denote the permutation describing the re-gluing of the slit plane: the upper edge of the rectangle $R_{i,j}$ is glued to the lower edge of $R_{i,\sigma_i(j)}$ (for $i = 0, 1, \ldots, q$; $j = 0, 1, \ldots, p-1$). And the left edge of $R_{i,j}$ is glued to the right edge of $R_{i+1,j}$ (for $i = 0, 1, \ldots, q-1$; $j = 0, 1, \ldots, p$).

We write a permutation σ as a product of its cycles, and a cycle sending i_0 to i_1, and i_1 to i_2, and so on, and i_l to i_0, is written from right to left, namely $\langle i_l, \ldots, i_2, i_1, i_0 \rangle$. For better readability we drop the commas between the one-digit numbers and write $\langle i_l \ \ldots \ i_2 \, i_1, \, i_0 \rangle$.

In our examples in Figure 3 these permutations are

$$\sigma_0 = \langle 4\,3\,2\,1\,0 \rangle, \qquad \sigma_1 = \langle 4\,1\,0 \rangle \langle 3\,2 \rangle, \qquad \sigma_2 = \langle 4\,1\,2\,3\,0 \rangle$$

and $\quad \sigma_0 = \langle 4\,3\,2\,1\,0 \rangle, \qquad \sigma_1 = \langle 4\,2\,1\,0 \rangle \langle 3 \rangle, \qquad \sigma_2 = \langle 4\,2\,0 \rangle \langle 1 \rangle \langle 3 \rangle,$

respectively.

Figures 4 and 5 show the gluing process in two steps. The example is the left hand side of Figure 3, a generic configuration with $g = 1$, $n = 1$ and $m = 0$, or Σ_1 from the list in Section 3.4. In Figure 4 the first slit pair is glued, producing a tube growing out of the complex plane; the second slit pair is still seen as two slits, one on the tube, one outside the tube. The gradient field of u is shown, with with two critical points S_1 and S_2.

Figure 5 shows the finished surface. The tube is with its later part re-glued into the plane, creating a plane with a handle. The point at infinity needs to be added.

3.4 The example $g = 1$, $n = 1$ and $m = 0$ geometrically

Here we want to give a complete list of all non-degenerate cells for the case $g = 1$, $m = 0$ and $n = 1$; this illustrates the explanations above and will be used later.

24	14 C	04
D		
23 A	13	03
B 22	D 12	02
C		
B 21	11	01
A		
20	10	00
σ_2	σ_1	σ_0

24	14 C	04
D		
23	13	03
D		
22 A	12 C	02
B		
B 21	11	01
A		
20	10	00
σ_2	σ_1	σ_0

Figure 3: The same two examples as in Figure 2, now shown with the grid pattern and the numbering of the rectangles; the example on the left is the cell Σ_1
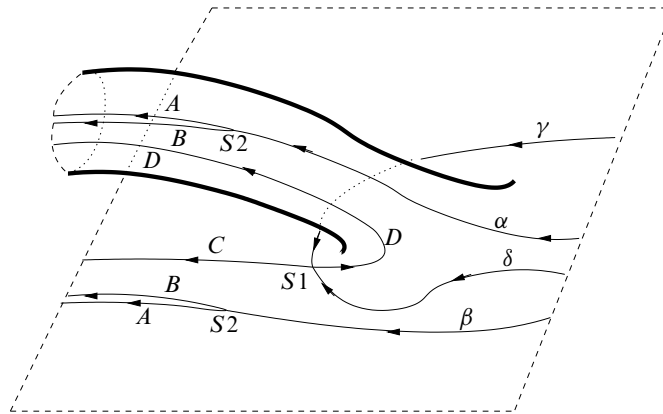

Figure 4: This shows the gluing in process: the surface is half-way finished

Figure 4 shows all eight non-degenerate cells $\Sigma_1, \dots, \Sigma_8$. Recall that a cell is an equivalence class of configurations; thus in each row we have drawn all configurations representing a cell.

Next we give the permutations of these eight cells. They will be used in Section 6 when we study this example algebraically.

For $(p, q) = (4, 2)$ there are two non-degenerate cells

$$\Sigma_1 = (\langle 41230 \rangle, \langle 32 \rangle \langle 410 \rangle, \langle 43210 \rangle) \quad \text{and} \quad \Sigma_2 = (\langle 41230 \rangle, \langle 21 \rangle \langle 430 \rangle, \langle 43210 \rangle).$$
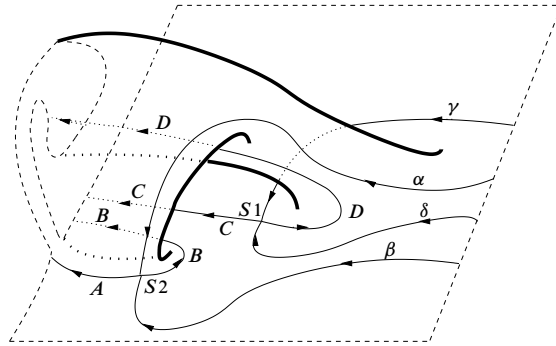
Figure 5: The finished surface

For $(p, q) = (4, 1)$ there is one non-degenerate cell

$$\Sigma_3 = (\langle 41230 \rangle, \langle 43210 \rangle).$$

For $(p, q) = (3, 2)$ there are three non-degenerate cells

$$\Sigma_4 = (\langle 3120 \rangle, \langle 2 \rangle \langle 310 \rangle, \langle 3210 \rangle),$$
$$\Sigma_5 = (\langle 3120 \rangle, \langle 320 \rangle \langle 1 \rangle, \langle 3210 \rangle),$$
$$\text{and} \quad \Sigma_6 = (\langle 3120 \rangle, \langle 21 \rangle \langle 30 \rangle, \langle 3210 \rangle).$$

For $(p, q) = (3, 1)$ there is one non-degenerate cell

$$\Sigma_7 = (\langle 3120 \rangle, \langle 3210 \rangle).$$

For $(p, q) = (2, 2)$ there is one non-degenerate cell

$$\Sigma_8 = (\langle 210 \rangle, \langle 20 \rangle \langle 1 \rangle, \langle 210 \rangle).$$

Note that the number of cells grows fast with g. In the next case $g = 2, n = 1, m = 0$ we have 17136 non-degenerate cells in dimensions 5 to 12.

4 The chain complexes $\mathbb{P}_{\bullet\bullet}$ and $\widetilde{\mathbb{P}}_{\bullet\bullet}$

Let h and m be fixed and set $n = 1$.

4.1 The cells

The cellular chain complex of the space $\mathrm{Par} = \widetilde{\mathrm{Par}}(h, m, n)$ is the total complex of a bi-graded complex $\mathbb{P}_{\bullet\bullet} = \bigoplus \mathbb{P}_{p,q}$, where $0 \leq p \leq 2h$ and $0 \leq q \leq h$. Here $\mathbb{P}_{p,q}$ is the
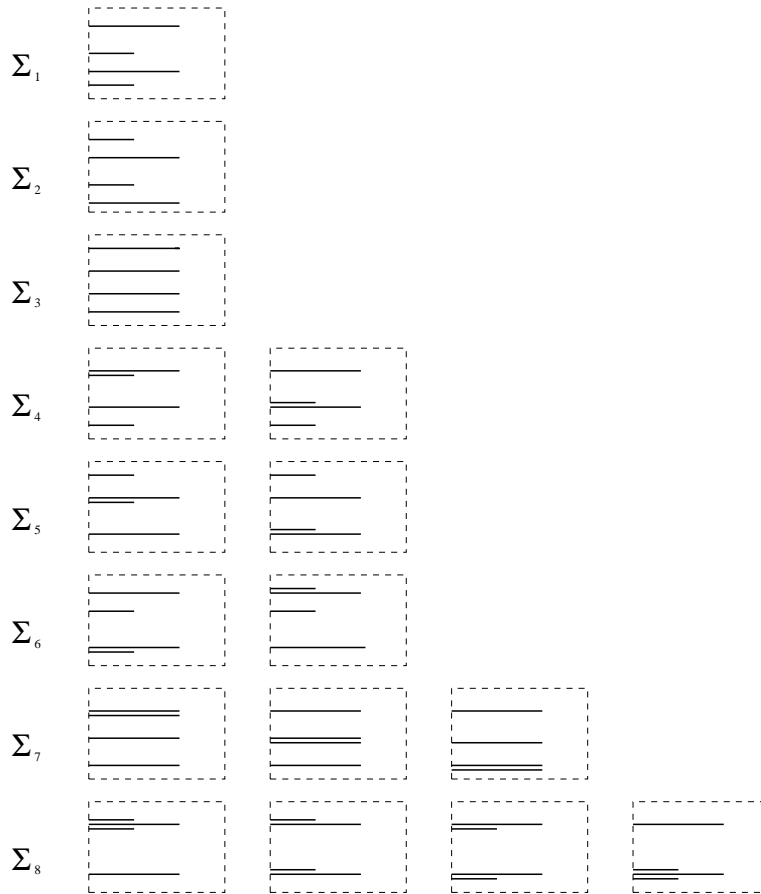
Figure 6: All eight cells for $g = 1$, $m = 0$ and $n = 1$: in each row the configurations representing this cell are shown

free abelian group generated by all $(q+1)$–tuples $\Sigma = (\sigma_q, \ldots, \sigma_0)$ of permutations σ_i in the symmetric group $\mathfrak{S}_{p+1}$, acting on $[p] = \{0, 1, \ldots, p\}$, and satisfying the following conditions:

$$(4\text{--}1) \qquad\qquad\qquad \mathrm{norm}(\Sigma) \leq h$$

$$(4\text{--}2) \qquad\qquad\qquad \mathrm{ncyc}(\sigma_q) \leq m + 1$$

Here the norm(Σ) is the sum of the word lengths,

$$\mathrm{norm}(\Sigma) = \ell(\sigma_q \sigma_{q-1}^{-1}) + \cdots + \ell(\sigma_1 \sigma_0^{-1}),$$

where the word length $\ell(\alpha)$ is measured with respect to the generating set of all transpositions in $\mathfrak{S}_{p+1}$. And $\mathrm{ncyc}(\alpha)$ is the number of cycles of a permutation α.

The cellular chain complex of the space $\widetilde{\mathrm{Par}}$ is the total complex of the bi-graded complex $\widetilde{\mathbb{P}}_{\bullet\bullet}$, where $\widetilde{\mathbb{P}}_{p,q}$ is generated by elements $(\nu; \Sigma) = (\nu; (\sigma_q, \dots, \sigma_0))$ where Σ is as before a $(q+1)$–tuple of permutations in $\mathfrak{S}_{p+1}$ satisfying the condition (4–1) and (4–2) above; and $\nu \colon [p] \to [m]$ is a function decoding a numbering of the punctures, which therefore must satisfy the following conditions:

(4–3) $\qquad\qquad\qquad$ ν is invariant under σ_q

(4–4) $\qquad\qquad\qquad$ ν induces a bijection $[p]/\sigma_q \to [m]$

(4–5) $\qquad\qquad\qquad$ $\nu(0) = \nu(p) = 0$

Here $[p]/\sigma_q$ denotes the set of σ_q–orbits in $[p]$.

4.2 The surface associated to a configuration

We repeat here the general construction we described for a generic configuration in Section 3.3

Given a cell Σ of bi-degree (p, q) and a point $a = (a_0, \dots, a_p)$ in a p–dimensional simplex Δ^p and a point $b = (b_0, \dots, b_q)$ in a q–dimensional simplex Δ^q we associate a surface $F = F(\Sigma; a, b)$ as follows. To begin, we identify the open unit interval with the real line, and thus interpret the a_i as real and the b_j as imaginary numbers.

Subdivide the complex plane by p horizontal lines at the a_i (respectively, by q vertical lines at the b_j) and number the $(p + 1)(q + 1)$ rectangles $R_{i,j}$ from bottom to top (respectively, from right to left). See the examples in Section 3.3.

If the rectangles $R_{i,j}$ along a column i are glued in cycles according to the permutation σ_i, and along a row according to their numbering, one obtains an "open" 2–complex which we compactify by adding a point Q_1 "at infinity" and at most m points $P_1, \dots, P_m$ at ends of the tubes created by the cycles of rectangles $R_{q,j}$; we denote this 2–complex by $F = F(\Sigma; a, b)$. Note that the $(p-1)(q-1)$ rectangles $R_{i,j}$ with $0 < i < q$ and $0 < j < p$ are now quadrilaterals on F, those with $i = 0, 0 < j < p$, $i = q, 0 < j < p$, $0 < i < q, j = 0$ or $0 < i < q, j = p$ are triangles (with one corner being Q_1) and the remaining four are two-gones with one corner being Q_1.

The definition of a degenerate configuration in Section 4.3 is made such F is a surface of genus exactly g with exactly m punctures if and only if Σ is non-degenerate. (Note that we use the term "degenerate" also for smooth F with genus or number of punctures smaller than expected.) Then we take F with the obvious complex structure and at

the point Q_1 we take the direction X_1 corresponding to the horizontal direction. Note that there is a harmonic function u given by projection to the real axis.

If F is a surface, but the genus is less than g or there are less than m punctures, then Σ will also be called degenerate.

4.3 Degenerate cells

The subcomplex $\mathbb{P}'$, which corresponds to the subspace Par$'$ of Par, consists of all Σ with norm less than h, or with a σ_q having less than $m+1$ cycles, or with any of the following conditions violated:

(4–6) $\sigma_i(p) = 0$ for $i = 0, \ldots, q$

(4–7) σ_0 is the rotation $\omega_p = \langle p, \ldots, 1, 0 \rangle$

(4–8) $\sigma_{i+1} \neq \sigma_i$ for $i = 0, \ldots, q$

(4–9)   There is no $0 \leq k \leq p-1$ such that $\sigma_i(k) = k+1$ for all $i = 0, \ldots, q$

The subcomplex $\widetilde{\mathbb{P}}'$, which corresponds to the subspace $\widetilde{\text{Par}}'$, consists of all cells $(\nu; \Sigma)$ with norm less than h, or with σ_q having less than $m+1$ cycles, or with ν not surjective, or with any of the conditions (4–3)–(4–5) or (4–6)–(4–9) violated.

Note that the first and the last faces of any cell under ∂' and ∂'' are degenerate.

The cells in $\widetilde{\text{Par}}'$ (respectively, in Par$'$) are called degenerate although the surfaces represented by their points might be smooth surfaces – but if so they have the wrong genus or the wrong number of punctures. Note that the map $\widetilde{\text{Par}} \to \text{Par}$, given by $(\nu; \Sigma) \mapsto \Sigma$, is only outside of $\widetilde{\text{Par}}'$ (respectively, Par$'$) a covering.

4.4 Vertical and horizontal boundary operator

The boundary operator $\partial = \partial' + (-1)^q \partial''$ on the complex $\mathbb{P}_{\bullet\bullet}$ is a sum of a vertical and a horizontal boundary operator, which are given by

(4–10) $\displaystyle \partial' = \sum_{i=0}^{q} (-1)^i \partial'_i$ with $\partial'_i(\Sigma) = (\sigma_q, \ldots, \widehat{\sigma}_i, \ldots, \sigma_0)$

(4–11) $\displaystyle \partial'' = \sum_{j=0}^{p} (-1)^j \partial''_j$ with $\partial''_j(\Sigma) = (D_j(\sigma_q), \ldots, D_j(\sigma_0))$.

Here $D_j \colon \mathfrak{S}_{p+1} \to \mathfrak{S}_p$ deletes the letter j from the cycle it occurs in and renormalizes the indices; more precisely, $D_j(\alpha) = s_j \circ \langle \alpha(j), j \rangle \circ \alpha \circ d_j$, where $d_j \colon [p-1] \to [p]$

is the simplicial degeneracy function which avoids the value j, and $s_i \colon [p] \to [p-1]$ is the simplicial face function which repeats the value i.

The boundary operator $\widetilde{\partial} = \widetilde{\partial}' + (-1)^q \widetilde{\partial}''$ on the complex $\widetilde{\mathbb{P}}_{\bullet\bullet}$ has the following terms. The vertical face operators do not act on the new data ν, thus

$$(4\text{--}12) \qquad \widetilde{\partial}'_i(\nu; \Sigma) = (\nu; \sigma_q, \ldots, \widehat{\sigma}_i, \ldots, \sigma_0).$$

For the horizontal face operators we need a deletion operator $\Delta_j(\nu) = \nu \circ d_j$ defined by composing ν with the simplicial degeneracy function $d_j \colon [p-1] \to [p]$ which avoids the value j. Then we define

$$(4\text{--}13) \qquad \widetilde{\partial}''_j(\nu; \Sigma) = (\Delta_j(\nu); D_j(\sigma_q), \ldots, D_j(\sigma_0)).$$

4.5 Homogeneous and inhomogeneous notation

It is convenient to have – apart from the homogeneous notation above – the inhomogeneous (or "bar") notation at hand: $\mathcal{T} = [\tau_q | \ldots | \tau_1]$ where $\tau_k := \sigma_k \cdot \sigma_{k-1}^{-1}$ is an element in $\mathfrak{S}_{p+1}$. Vice versa, $\sigma_k := \tau_k \cdots \tau_1 \cdot \omega$. The norm $\mathrm{norm}(\mathcal{T}) = \ell(\tau_q) + \cdots + \ell(\tau_1) \le h$, and the number of cycles $\mathrm{ncyc}(\mathcal{T}) = \mathrm{ncyc}(\sigma_q) = \mathrm{ncyc}(\tau_q \cdots \tau_1 \cdot \omega) \le m+1$. The conditions translate now into $\tau_k(0) = 0$ for $k = 1, \ldots, q$, $\tau_k \ne \mathbb{1}$ for $k = 1, \ldots, q$, and that there is now common fixed point of all τ_k, except 0.

The vertical face operators are now $\partial'_i(\mathcal{T}) = [\tau_q | \ldots | \tau_{i+1}\tau_i | \ldots]$, for $i = 1, \ldots, q-1$, and are set equal to 0 for $i = 0, q$. The horizontal face operators translate into corresponding operators $\partial''_j(\mathcal{T})$.

In the non-permutable case, all conditions on the puncture enumeration ν must be expressed as before.

5 Some properties of the chain complexes $\mathbb{P}_{\bullet\bullet}$ and $\widetilde{\mathbb{P}}_{\bullet\bullet}$

Let h, $m \ge 0$ be fixed, and set $n = 1$.

5.1 The complexes $\mathbb{P}_{\bullet\bullet}$

The spaces Par (respectively, $\widetilde{\mathrm{Par}}$) are the geometric realizations of the bi-semi-simplicial complexes consisting of all the cells, degenerate or not.

The degenerate cells form a subcomplex Par' resp $\widetilde{\mathrm{Par}}'$. Thus they are finite cell complexes whose cells are products $\Delta^p \times \Delta^q$ of simplices, where $p = 0, 1, \ldots, 2h$ and $q = 0, 1, \ldots, h$. All cells of dimension less then $h+2$, in particular all 0–cells, are contained in Par' (respectively, in $\widetilde{\mathrm{Par}}'$).

We remark here that a subcomplex of Par is contractible. Namely, if we change the definition of the norm by adding the term $\mathrm{norm}(\sigma_0 \omega^{-1})$, we have the same non-degenerate cells, but fewer degenerate cells. The complement of these degenerate cells is still homeomorphic to the space $\mathfrak{Harm}$. After this modification we would have $H^{*-1}(\mathrm{Par}') \cong H_{3h-*}(\mathfrak{Mod})$. We will investigate this in a forthcoming article exhibiting $\mathfrak{Mod}$ as the interior of a compact manifold with boundary.

5.2 The quotient complex

Since the subcomplex $\mathbb{P}'_{\bullet\bullet}$ is generated by basis elements, the quotient complex $\mathbb{Q}_{\bullet\bullet} := \mathbb{P}_{\bullet\bullet}/\mathbb{P}'_{\bullet\bullet}$ is generated by all Σ not in the subcomplex; and the face operators ∂'_i (respectively, ∂''_j) are set to be zero if they land in the subcomplex. In particular $\partial'_0 = \partial'_q = 0$ and $\partial''_0 = \partial''_p = 0$, since they always reduce the norm or the number of punctures or violate any of the condition stated.

Similar statements hold for the chain complex $\widetilde{\mathbb{Q}}_{\bullet\bullet} := \widetilde{\mathbb{P}}_{\bullet\bullet}/\widetilde{\mathbb{P}}'_{\bullet\bullet}$.

5.3 The spectral sequence of the double complex

The double complex $\mathbb{Q}_{\bullet\bullet}$ gives rise to a spectral sequence starting with the E^0–term $E^0_{p,q} = \mathbb{Q}_{p,q}$. It is concentrated in the first quadrant in the rectangle $0 \le p \le 2h$ and $0 \le q \le h$; moreover, $E^0_{p,q} = 0$ for $p = 0, 1$ and for $pq \le h$.

It turns out that (for fixed p) the vertical homology $E^1_{p,q} = H_q(\mathbb{Q}_{p,\bullet}, \partial')$ is concentrated in the maximal degree $q = h$. Thus the E_1–term is a chain complex with differential induced by ∂''. And the spectral sequence collapses with $E^2 = E^\infty$.

5.4 The bar resolution

For fixed p the chain complex $\mathbb{P}_{p,\bullet}$ is similar to the homogeneous bar resolution of the group $\mathfrak{S}_p$. First, since we require $\sigma_i(p) = 0$ for the permutations $\sigma_i \in \mathfrak{S}_{p+1}$, they are actually in one-to-one correspondence with $\mathfrak{S}_p$. Secondly, to normalize $\sigma_0 = \omega_p = \langle 0, 1, \ldots, p \rangle$ amounts to taking the coefficient module $\mathbb{Z}$ with trivial $\mathfrak{S}_p$ action. If one filters the bar resolution by the norm, then $\mathbb{P}_{p,\bullet}(h, m, 1)$ is a summand in the hth filtration quotient, namely the summand determined by σ_q having $m + 1$ cycles.

Note that each cell Σ intersects the subspace Par' of degenerate surfaces; more precisely, in the quotient chain complex $\mathbb{Q}_{\bullet\bullet}$ we have $\partial'_0(\Sigma) = \partial'_q(\Sigma) = 0$ and $\partial''_0(\Sigma) = \partial''_p(\Sigma) = 0$ for a cell Σ of bi-degree (p, q).

Similar statements hold for the chain complex $\widetilde{\mathbb{Q}}_{p,\bullet}$.

6 The example $g = 1$, $n = 1$ and $m = 0$ algebraically

In this section we discuss the example $g = 1$, $m = 0$ and $n = 1$, the moduli space of tori with one boundary curve and no punctures. Thus $d + c = 6$. The possible values for p are $p = 0, 1, 2, 3, 4$, and for q they are $q = 0, 1, 2$. We write the cells in the homogeneous notation.

6.1 The cells

Recall the eight non-degenerate cells $\Sigma_1, \ldots, \Sigma_8$ as given above in Section 3.4. With bi-degrees

$$(p, q) = (4, 2) : \Sigma_1 \text{ and } \Sigma_2 \text{ in dimension } 6$$
$$(p, q) = (4, 1) : \Sigma_3 \text{ in dimension } 5$$
$$(p, q) = (3, 2) : \Sigma_4, \Sigma_5 \text{ and } \Sigma_6 \text{ in dimension } 5$$
$$(p, q) = (3, 1) : \Sigma_7 \text{ in dimension } 4$$
$$(p, q) = (2, 2) : \Sigma_8 \text{ in dimension } 4$$

6.2 The E^0–term

The E^0–term is shown in the following table:

(6–1)

$q = 2$			Σ_8	$\Sigma_4, \Sigma_5, \Sigma_6$	Σ_1, Σ_2
$q = 1$				Σ_7	Σ_3
$q = 0$					
	$p = 0$	$p = 1$	$p = 2$	$p = 3$	$p = 4$

The vertical boundary operator ∂' is

$$\partial'(\Sigma_1) = \partial'(\Sigma_2) = -\Sigma_3, \qquad \partial'(\Sigma_4) = \partial'(\Sigma_5) = \partial'(\Sigma_6) = -\Sigma_7.$$

6.3 The E^1–term

We set $A := \Sigma_1 - \Sigma_2$, $B := \Sigma_4 - \Sigma_5$, and $C := \Sigma_4 - \Sigma_6$. Note that in this example the fundamental class (see Section 7) is $\mu = -A$.

Then the E^1–term is as follows:

(6–2)

$q = 2$			Σ_8	B, C	A
$q = 1$				0	0
$q = 0$					
	$p = 0$	$p = 1$	$p = 2$	$p = 3$	$p = 4$

The horizontal boundary operator ∂'' is

$$\partial''(A) = 0, \qquad \partial''(B) = -2\Sigma_8, \qquad \partial''(C) = -\Sigma_8.$$

6.4 The E^2–term and final result

If we set $D := B - 2C$ we have a cycle in degree $(3, 2)$, and therefore an E^2–term as follows:

(6–3)

	$p=0$	$p=1$	$p=2$	$p=3$	$p=4$
$q=2$			0	D	A
$q=1$				0	0
$q=0$					

The moduli space of tori with one boundary curve is orientable and homotopy-equivalent to the complement of the trefoil knot in $\mathbb{R}^3$, or in other words the mapping class group Γ is isomorphic to the third braid group; its cohomology is infinite cyclic in degrees 0 and 1.

7 The fundamental class

Here we set $n = 1$. Then $h = 2g + m$. The (relative) cycle μ representing the fundamental class $[\mu] \in H_{3h}(\mathbb{P}, \mathbb{P}'; \mathbb{Z})$ is given as follows. First, its degree is $(p, q) = (2h, h)$. Thus we need $2h$ permutations $\tau_h, \ldots, \tau_1$ for the inhomogeneous notation. We set $\tau_1 = \langle 3, 1 \rangle$ and $\tau_2 = \langle 4, 2 \rangle$, an interlocking pair of disjoint transpositions. We continue in this way until we have g blocks of two pairs of interlocking transpositions. Then we continue with $\tau_{2g+1} = \langle 4g+2, 4g+1 \rangle$, till $\tau_{2g+m} = \langle 4g+2m, 4g+2m-1 \rangle$; these are m neighbour transpositions.

Altogether we have $2h$ disjoint (and therefore commuting) transpositions. The g *symplectic pairs* of interlocking transpositions create each a handle of the surface; and the m non-interlocking transpositions create each a puncture. The cycle number of $\tau_h \cdots \tau_1 \cdot \omega_{2h}$ is $m + 1$.

Let $\Lambda(h, m)$ denote the subset of all permutations $\alpha \in \mathfrak{S}_{2h}$ such that the horizontally conjugated cell

(7–1) $$\kappa_\alpha(T) = [\alpha\tau_h\alpha^{-1}| \ldots |\alpha\tau_1\alpha^{-1}]$$

has the same cycle number $\mathrm{ncyc}(\alpha.T) = m + 1$. Furthermore, for $\pi \in \mathfrak{S}_h$ let

(7–2) $$\pi.T = [\tau_{\pi(h)}| \ldots |\tau_{\pi(1)}]$$

denote the vertically permuted cell. These operations were studied by Schardt [34]. The chain

$$(7\text{--}3) \qquad \mu = \sum_{\pi \in \mathfrak{S}_h} \sum_{\alpha \in \Lambda(h,m)} \text{sign}(\pi)\,\text{sign}(\alpha)\ \pi\,.\,\kappa_\alpha(T)$$

is a cycle and represents the fundamental class. For example, when $g = 2, m = 0$, this cycle has 504 terms.

8 The orientation system

The local coefficient system is the orientation system of the relative manifold Par, Par$'$. For $m \geq 2$ it is not trivial, see Müller [30]. In order to determine the change of sign along a path, we can restrict to edge paths from barycenters to barycenters in a subdivision.

We will associate to each cell $\mathcal{T}$ a top-dimensional cell $\text{top}(\mathcal{T})$. Denote then by $\epsilon(\mathcal{T})$ the sign with which $\text{top}(\mathcal{T})$ occurs in the fundamental class μ. The sign change for the path from the barycenter of $\mathcal{T}$ to the barycenter of $\mathcal{T}'$, where $\mathcal{T}' \subset \mathcal{T}$, is then the product $\epsilon(\mathcal{T})\epsilon(\mathcal{T}')$ of these two signs.

To define the cell $\text{top}(\mathcal{T})$ we associate to $\mathcal{T} = [\tau_q | \ldots | \tau_1]$ we start by writing each τ_i in a certain normal form $\text{NF}(\tau_i)$. First, if $\alpha = \langle i_l, \ldots, i_0 \rangle$ is a permutation consisting of just one cycle, we write it as $\alpha = \text{NF}(\alpha) = \langle i_l, i_{l-1} \rangle \cdot \cdots \cdot \langle i_1, i_0 \rangle$. If α consists of several (non-trivial) cycles, we order them by their minima, the absolute minimum being first (or in our notation rightmost). This gives a normal form

$$(8\text{--}1) \qquad \alpha = \text{NF}(\alpha) = \cdots \cdot \langle i'_{l'}, i'_{l'-1} \rangle \cdot \cdots \cdot \langle i'_1, i'_0 \rangle \cdot \langle i_l, i_{l-1} \rangle \cdot \cdots \cdot \langle i_1, i_0 \rangle.$$

Assume we have the normal forms $\text{NF}(\tau_q), \ldots, \text{NF}(\tau_1)$. The next step is to "separate" the factors in each normal form $NF(\tau_i)$ by replacing all product signs by a bar symbol. We obtain a new cell:

$$(8\text{--}2) \qquad \mathcal{T}' = [\theta_h \,|\, \theta_{h-1} \,|\, \ldots \,|\, \theta_1].$$

Note that it has exactly h transpositions $\theta_h, \ldots, \theta_1$. Thus $\mathcal{T}$ has bi-degree (p, h) (and is not yet the top-dimensional cell we seek).

The next step is to "spread out" these transpositions, that is to replicate indices if they occur in several of the transpositions. Denote for $j = 0, \ldots, p$ by $S_j \colon \mathfrak{S}_p \to \mathfrak{S}_{p+1}$ the function which sends the permutation α to the new permutation $S_j(\alpha)$ by increasing the indices $k \geq j$ in a cycle notation to $k + 1$ and leaving the others. Note that j becomes a fixed point. In other words, $S_j(\alpha) = d_j \circ \langle \alpha(j), j \rangle \circ \alpha \circ s_j$ expressed with

the simplicial face and degeneracy maps. (See the definition of D_j in Section 4.2; note that neither the D_j nor the S_j are group homomorphisms; they turn the family of symmetric groups into a crossed simplicial group.) Since $S_j(\langle k, l \rangle) = \langle d_j(k), d_j(l) \rangle$, a transposition is mapped to a transposition.

Assume k is the lowest index in $\mathcal{T}'$ occurring more than ones in one of transpositions θ_i, say in θ_{i_1} the first time and in θ_{i_2} the second time, for $i_2 > i_1$. Then we replace $\mathcal{T}'$ by

$$(8\text{--}3) \quad \mathcal{T}'' = [S_k(\theta_h)|S_k(\theta_{h-1})|\ldots|S_k(\theta_{i_2})|\ldots|S_k(\theta_{i_1+1})|S_{k+1}(\theta_{i_1})|\ldots|S_{k+1}(\theta_1)],$$

a cell of bi-degree $(p+1, h)$. We repeat this last step until no index occurs more than ones in these transpositions, each time raising the first degree by one. The final result is a sequence of h disjoint transpositions, thus a cell $\mathrm{top}(\mathcal{T})$ of degree $(2h, h)$.

9 Comments on the computation

The C++ program with documentation is contained in the first author's thesis [1]. It is about 3000 lines long and consists of 187 subroutines. Here we give some comments.

9.1 Listing the cells

The computer program uses the C++ Standard Template Library extensively. A permutation in $\mathfrak{S}_{p+1}$ is implemented as a vector of integers (list of values) and also as a single integer using an easy computable bijection $\mathfrak{S}_{p+1} \to \{1, \ldots, (p+1)!\}$. Thus manipulations can be performed easily and an efficient storage handling is possible up to $h = 6$.

We obtain the non-degenerate cells or generators of $\mathbb{Q}_{\bullet\bullet}$ by first generating the set Λ of all cells in bi-degree $(2h, h)$, namely all h–tuples of disjoint transpositions in $\mathfrak{S}_{2h}$ – there are $L_h = (2h-1)!! = \frac{(2h)!}{2^h h!}$ such tuples – then we sort them according to their cycle number m into sets $\Lambda(h, m)$. Note that for h odd (respectively, even) the cycle number m is again odd (respectively, even).

Applying the vertical boundary operator ∂' successively gives all generators of the chain complex $\mathbb{Q}_{2h, \bullet}$. Next we generate the cells of bi-degree $(2h-1, h)$ as images of the cells of bi-degree $(2h, h)$ under the horizontal boundary operator ∂''. Inductively, we obtain all cells of $\mathbb{Q}_{\bullet\bullet}$.

The same procedure gives the cells of the complex $\widetilde{\mathbb{Q}}_{\bullet\bullet}$, where we store all possible puncture enumerations $\nu \colon [p] \to [m]$ additionally.

9.2   The matrices of the boundary operator

While generating the cells, the matrices D' resp D'' of the two boundary operators ∂' (respectively, ∂'') are produced simultaneously. We store the matrices in the following sparse format: for the matrix entries, a compressed row format is used; moreover, a compressed column matrix of boolean variables gives the positions of the nonzero entries. This seems to be a reasonable trade-off between memory space and running time, because both row and column operations are performed frequently on the matrix.

For the homology of the complex $\mathbb{Q}_{\bullet\bullet}$ (respectively, $\widetilde{\mathbb{Q}}_{\bullet\bullet}$) we first compute the Smith normal forms of the matrices of the vertical boundary operators. As noted earlier, for each p, the homology of the vertical chain complexes $\mathbb{Q}_{p,\bullet}$ is just the kernel of $\partial'\colon \mathbb{Q}_{p,h} \to \mathbb{Q}_{p,h-1}$. This gives the E^1–term of the spectral sequence.

In order to compute its E_2–term and thus the desired homology of the total complex, we add a lattice reduction routine, the LLL-algorithm (named after Lenstra-Lenstra-Lovász) while computing the Smith normal form (or elementary divisors) of the horizontal boundary operator ∂''. This is important to avoid a coefficient explosion in the case $h = 5$. All the computations were also done modulo 2.

9.3   Size of the matrices

Both running time and memory space grow exponentially with h. More precisely, let $N_{p,q} = N_{p,q}(h,m)$ be the number of cells of bi-degree (p,q). Table 1 shows these numbers for some cases.

Ranks of the E^0–term for $h = 5$ and $q = 5, 4$ Observe that both boundary operators leave the puncture number m invariant, so we can compute the homology for each $m \equiv h \mod 2$ separately.

To generate the matrix $D'_{p,q}$ or $D''_{p,q}$ of a boundary operator $\partial'\colon \mathbb{Q}_{p,q} \to \mathbb{Q}_{p,q-1}$ (respectively, $\partial''\colon \mathbb{Q}_{p,q} \to \mathbb{Q}_{p-1,q}$) we need to take $q-1$ (respectively, $p-1$) boundary faces from $N_{p,q}$ cells and search these face cells in a (sorted) list of $N_{p,q-1}$ resp $N_{p-1,q}$ cells. This leads to a running time of $O(hN^2 \log N)$, where $N = \max\{N_{p,q}\}$. We only need to compute the matrices $D'_{2,h}, \ldots, D'_{2h,h}$ and $D''_{3,h}, \ldots, D''_{2h,h}$. See Table 1 for the size of the matrices $D'_{p,5}$ for $h = 5$.

The most time-consuming procedure when determining the Smith normal form is the LLL-algorithm. This algorithm, applied to r columns of an integer matrix takes $O(r^6 \log^3 B)$ steps, where B is the maximal norm of a column. But note that we apply the LLL-algorithm only when the coefficients exceed a prescribed barrier, and also only to portions of the columns, so r is much smaller than N.

$p=$	0	1	2	3	4	5	6	7	8	9	10
$h=5$ $m=1$											
$q=5$	0	0	1	240	6170	51115	195264	394240	435680	249480	57960
$q=4$	0	0	0	216	7840	76140	320880	694148	808192	482328	115920
$h=5$ $m=3$											
$q=5$	0	0	0	0	640	12425	74610	202825	278600	189000	50400
$q=4$	0	0	0	0	800	18500	122700	357280	516880	365400	100800
$h=5$ $m=5$											
$q=5$	0	0	0	0	0	0	1296	7735	16520	15120	5040
$q=4$	0	0	0	0	0	0	2160	13692	30688	29232	10080

Table 1: Ranks of the E^0–term for $h=5$ and $q=5,4$

Ranks of the E^1–term for $h=5$ The most memory-consuming part in the computation procedure is the storage of the matrices $D''_{p,h}$ for the horizontal boundary operator ∂''. in terms of the transformed basis. Numerical values for the number of generators of the E_1–term can again be taken from Table 2 giving estimates for the matrix sizes $D''_{p,5}$.

$p=$	0	1	2	3	4	5	6	7	8	9	10
$h=5$ $m=1$											
$q=5$	0	0	1	60	650	2860	6588	8708	6678	2772	483
$h=5$ $m=3$											
$q=5$	0	0	0	0	70	700	2520	4480	4270	2100	420
$h=5$ $m=5$											
$q=5$	0	0	0	0	0	0	1	14	56	84	42

Table 2: Ranks of the E^1–term for $h=5$

We were able to compute the homology of the complexes $\mathbb{Q}_{\bullet\bullet}$ up to $h=5$ on a machine with 4 GB of RAM and a 3 GHz processor taking approximately 4 days for the case $h=5$, $m=1$. The computational problems for $h>5$ are both running time and memory space.

References

[1] **J Abhau**, *Die Homologie von Modulräumen Riemannscher Flächen – Berechnungen für g ≤ 2*, Diplom thesis, Universität Bonn (2005)

[2] **V I Arnol'd**, *The cohomology ring of the group of dyed braids*, Mat. Zametki 5 (1969) 227–231 MR0242196

[3] **V I Arnol'd**, *Certain topological invariants of algebrac functions*, Trudy Moskov. Mat. Obšč. 21 (1970) 27–46 MR0274462

[4] **D J Benson**, **F R Cohen**, *Mapping class groups of low genus and their cohomology*, Mem. Amer. Math. Soc. 90 (1991) iv+104 MR1052554

[5] **C-F Bödigheimer**, *The Hilbert uniformization I*, in preparation

[6] **C-F Bödigheimer**, *The topology of moduli spaces, part I: Hilbert uniformization*, Math. Gott. Preprint Series SFB 170 9 (1990)

[7] **C-F Bödigheimer**, *Configuration models for moduli spaces of Riemann surfaces with boundary*, Abh. Math. Sem. Univ. Hamburg 76 (2006) 191–233 MR2293442

[8] **C-F Bödigheimer**, **F R Cohen**, **M D Peim**, *Mapping class groups and function spaces*, from: "Homotopy methods in algebraic topology (Boulder, CO, 1999)", Contemp. Math. 271, Amer. Math. Soc., Providence, RI (2001) 17–39 MR1831345

[9] **F Cohen**, *Cohomology of braid spaces*, Bull. Amer. Math. Soc. 79 (1973) 763–766 MR0321074

[10] **F Cohen**, *The homology of C_{n+1}-spaces, $n \geq 0$*, from: "The Homology of Iterated Loop Spaces", (F R Cohen, T J Lada, J P May, editors), Lecture Notes in Mathematics 533, Springer (1976) 207–353

[11] **J Ebert**, *The Hilbert uniformization II*, in preparation

[12] **J Ebert**, *Über den Modulraum mehrfach gerichteter und punktierter Kleinscher Flächen*, Diplom thesis, Universität Bonn (2003)

[13] **R Ehrenfried**, *Die Homologie der Modulräume berandeter Riemannscher Flächen von kleinem Geschlecht*, Bonner Mathematische Schriften 306, Universität Bonn Mathematisches Institut, Bonn (1998) MR1938981 PhD thesis, Universität Bonn (1997)

[14] **D B Fuks**, *Cohomology of the braid group* mod 2, Funkcional. Anal. i Priložen. 4 (1970) 62–73 MR0274463

[15] **S Galatius**, *Mod p homology of the stable mapping class group*, Topology 43 (2004) 1105–1132 MR2079997

[16] **H Glover**, **G Mislin**, *Torsion in the mapping class group and its cohomology*, from: "Proceedings of the Northwestern conference on cohomology of groups (Evanston, Ill., 1985)", volume 44 (1987) 177–189 MR885103

[17] **V Godin**, *The unstable integral homology of the mapping class groups of a surface with boundary*, Math. Ann. 337 (2007) 15–60 MR2262776

[18]　**J Harer**, *The second homology group of the mapping class group of an orientable surface*, Invent. Math. 72 (1983) 221–239　MR700769

[19]　**J L Harer**, *Stability of the homology of the mapping class groups of orientable surfaces*, Ann. of Math. (2) 121 (1985) 215–249　MR786348

[20]　**J L Harer**, *The virtual cohomological dimension of the mapping class group of an orientable surface*, Invent. Math. 84 (1986) 157–176　MR830043

[21]　**J L Harer**, *The cohomology of the moduli space of curves*, from: "Theory of moduli (Montecatini Terme, 1985)", Lecture Notes in Math. 1337, Springer, Berlin (1988) 138–221　MR963064

[22]　**J Harer**, *The third homology group of the moduli space of curves*, Duke Math. J. 63 (1991) 25–55　MR1106936

[23]　**N V Ivanov**, *Mapping class groups*, from: "Handbook of geometric topology", North-Holland, Amsterdam (2002) 523–633　MR1886678

[24]　**M Korkmaz**, *First homology group of mapping class groups of nonorientable surfaces*, Math. Proc. Cambridge Philos. Soc. 123 (1998) 487–499　MR1607985

[25]　**M Korkmaz**, *Low-dimensional homology groups of mapping class groups: a survey*, Turkish J. Math. 26 (2002) 101–114　MR1892804

[26]　**M Korkmaz**, **A I Stipsicz**, *The second homology groups of mapping class groups of oriented surfaces*, Math. Proc. Cambridge Philos. Soc. 134 (2003) 479–489　MR1981213

[27]　**E Looijenga**, *Cohomology of $\mathcal{M}_3$ and $\mathcal{M}_3^1$*, from: "Mapping class groups and moduli spaces of Riemann surfaces (Göttingen, 1991/Seattle, WA, 1991)", Contemp. Math. 150, Amer. Math. Soc., Providence, RI (1993) 205–228　MR1234266

[28]　**I Madsen**, **M Weiss**, *The stable moduli space of Riemann surfaces: Mumford's conjecture* `arXiv:math.AT/0212321`

[29]　**S Morita**, *Families of Jacobian manifolds and characteristic classes of surface bundles I*, Ann. Inst. Fourier (Grenoble) 39 (1989) 777–810　MR1030850

[30]　**M Müller**, *Orientierbarkeit des Raumes der Parallelschlitzgebiete*, Diplom thesis, Universität Bonn (1996)

[31]　**D Mumford**, *Abelian quotients of the Teichmüller modular group*, J. Analyse Math. 18 (1967) 227–244　MR0219543

[32]　**W Pitsch**, *Un calcul élémentaire de $H_2(\mathcal{M}_{g,1}, \mathbb{Z})$ pour $g \geq 4$*, C. R. Acad. Sci. Paris Sér. I Math. 329 (1999) 667–670　MR1724094

[33]　**J Powell**, *Two theorems on the mapping class group of a surface*, Proc. Amer. Math. Soc. 68 (1978) 347–350　MR0494115

[34]　**S Schardt**, *Die Hopf-Struktur auf der Konjugation-Shuffle-Algebra der symmetrischen Gruppen*, Diplom thesis, Universität Bonn (2003)

[35] **O Tommasi**, *Rational cohomology of the moduli space of genus 4 curves*, Compos. Math. 141 (2005) 359–384 MR2134272

[36] **O Tommasi**, *Rational cohomology of* $\mathcal{M}_{3,2}$, Compos. Math. 143 (2007) 986–1002 MR2339836

[37] **F V Vaĭnšteĭn**, *The cohomology of braid groups*, Funktsional. Anal. i Prilozhen. 12 (1978) 72–73 MR498903

[38] **M Zaw**, *The moduli space of non-classical directed Klein surfaces*, Bonner Mathematische Schriften 313, Universität Bonn Mathematisches Institut, Bonn (1998) MR1933809 PhD thesis, Universität Bonn (1998)

Mathematisches Institut, Universität Bonn
Beringstraße 1, D–53115 Bonn, Germany

boedigheimer@math.uni-bonn.de